NASA/TM—2001-107181

Parametric Data From a Wind Tunnel Test on a Rocket-Based Combined-Cycle Engine Inlet

René Fernandez, Charles J. Trefny, and Scott R. Thomas
Glenn Research Center, Cleveland, Ohio

Mel J. Bulman
Gencorp Aerojet Corporation, Sacramento, California

November 2001

The NASA STI Program Office . . . in Profile

Since its founding, NASA has been dedicated to the advancement of aeronautics and space science. The NASA Scientific and Technical Information (STI) Program Office plays a key part in helping NASA maintain this important role.

The NASA STI Program Office is operated by Langley Research Center, the Lead Center for NASA's scientific and technical information. The NASA STI Program Office provides access to the NASA STI Database, the largest collection of aeronautical and space science STI in the world. The Program Office is also NASA's institutional mechanism for disseminating the results of its research and development activities. These results are published by NASA in the NASA STI Report Series, which includes the following report types:

- TECHNICAL PUBLICATION. Reports of completed research or a major significant phase of research that present the results of NASA programs and include extensive data or theoretical analysis. Includes compilations of significant scientific and technical data and information deemed to be of continuing reference value. NASA's counterpart of peer-reviewed formal professional papers but has less stringent limitations on manuscript length and extent of graphic presentations.

- TECHNICAL MEMORANDUM. Scientific and technical findings that are preliminary or of specialized interest, e.g., quick release reports, working papers, and bibliographies that contain minimal annotation. Does not contain extensive analysis.

- CONTRACTOR REPORT. Scientific and technical findings by NASA-sponsored contractors and grantees.

- CONFERENCE PUBLICATION. Collected papers from scientific and technical conferences, symposia, seminars, or other meetings sponsored or cosponsored by NASA.

- SPECIAL PUBLICATION. Scientific, technical, or historical information from NASA programs, projects, and missions, often concerned with subjects having substantial public interest.

- TECHNICAL TRANSLATION. English-language translations of foreign scientific and technical material pertinent to NASA's mission.

Specialized services that complement the STI Program Office's diverse offerings include creating custom thesauri, building customized data bases, organizing and publishing research results . . . even providing videos.

For more information about the NASA STI Program Office, see the following:

- Access the NASA STI Program Home Page at ***http://www.sti.nasa.gov***

- E-mail your question via the Internet to help@sti.nasa.gov

- Fax your question to the NASA Access Help Desk at 301–621–0134

- Telephone the NASA Access Help Desk at 301–621–0390

- Write to:
  NASA Access Help Desk
  NASA Center for AeroSpace Information
  7121 Standard Drive
  Hanover, MD 21076

NASA/TM—2001-107181

Parametric Data From a Wind Tunnel Test on a Rocket-Based Combined-Cycle Engine Inlet

René Fernandez, Charles J. Trefny, and Scott R. Thomas
Glenn Research Center, Cleveland, Ohio

Mel J. Bulman
Gencorp Aerojet Corporation, Sacramento, California

Prepared for the
1995 Airbreathing Propulsion Subcommittee Meeting
sponsored by the Joint Army-Navy-NASA-Air Force Interagency Propulsion Committee
Tampa, Florida, December 5–9, 1995

National Aeronautics and
Space Administration

Glenn Research Center

November 2001

Available from

NASA Center for Aerospace Information
7121 Standard Drive
Hanover, MD 21076

National Technical Information Service
5285 Port Royal Road
Springfield, VA 22100

Available electronically at http://gltrs.grc.nasa.gov/GLTRS

PARAMETRIC DATA FROM A WIND TUNNEL TEST ON A ROCKET- BASED COMBINED-CYCLE ENGINE INLET

René Fernandez, Charles J. Trefny, and Scott R. Thomas
National Aeronautics and Space Administration
Glenn Research Center
Cleveland, Ohio 44135

Mel J. Bulman
Gencorp Aerojet Corporation
Sacramento, California 95813–6000

SUMMARY

A 40-percent scale model of the inlet to a rocket-based combined-cycle (RBCC) engine was tested in the NASA Glenn Research Center 1- by 1-Foot Supersonic Wind Tunnel (SWT). The full-scale RBCC engine is scheduled for test in the Hypersonic Tunnel Facility (HTF) at NASA Glenn's Plum Brook Station at Mach 5 and 6. This engine will incorporate the configuration of this inlet model which achieved the best performance during the present experiment. The inlet test was conducted at Mach numbers of 4.0, 5.0, 5.5, and 6.0. The fixed-geometry inlet consists of an 8° forebody compression plate, boundary layer diverter, and two compressive struts located within 2 parallel side-walls. These struts extend through the inlet, dividing the flowpath into three channels. Test parameters investigated included strut geometry, boundary layer ingestion, and Reynolds number (Re). Inlet axial pressure distributions and cross-sectional Pitot-pressure surveys at the base of the struts were measured at varying back-pressures. Inlet performance and starting data are presented. The inlet chosen for the RBCC engine self-started at all Mach numbers from 4 to 6. Pitot-pressure contours showed large flow nonuniformity on the body-side of the inlet. The inlet provided adequate pressure recovery and flow quality for the RBCC cycle even with the flow separation.

NOMENCLATURE

A_d	boundary layer diverter freestream flow area
A_i	inlet capture area
A_o	freestream captured stream tube area
M_4	mass averaged Mach number at the end of the struts
M_o	freestream Mach
p_s	model static pressure
p_{so}	freestream static pressure
p_{TO}	freestream total pressure
T_{TO}	freestream total temperature
η_{pt}	mass averaged total pressure recovery
η_{KE}	mass averaged kinetic energy efficiency
γ	gamma, ratio of specific heats, 1.4

BACKGROUND AND INTRODUCTION

Rocket-based combined-cycle (RBCC) engines combine the high thrust-to-weight ratio of rockets with the high specific impulse of ramjets in a single, integrated propulsion system that is capable of generating thrust from sea-level-static to high Mach number conditions. The "strutjet" (ref. 1) is one example of this engine concept which is being developed cooperatively by a government-industry team.

The strutjet is an ejector-ramjet engine in which small, fuel-rich rocket chambers are embedded into the trailing edges of the inlet compression struts. The engine operates as an ejector-ramjet from take-off to about

Mach 3. At low Mach number, entrained air is completely consumed by the fuel-rich rocket exhaust. As freestream Mach number and airflow increase, additional fuel is introduced to maintain the stoichiometric combustion of all available oxygen. At approximately Mach 3 the strut rockets are turned off. From Mach 3 to 6, the engine operates as a thermally-choked ramjet, and then transitions to supersonic-combustion (scramjet) mode at about Mach 6. For space-launch applications, the rockets are re-ignited at a Mach number beyond which air-breathing propulsion becomes impractical.

A strutjet engine test article, designed for up to Mach 8 cruise on hydrocarbon fuel, is currently being developed and will be tested initially at the Hypersonic Tunnel Facility (HTF) free-jet at the NASA Plum Brook Station (ref. 2). To properly match Mach 6 and 7 freestream flight conditions and simulate vehicle forebody compression, Mach 5 and 6 nozzles will be used at Mach 6 and 7 enthalpy levels. Figure 1 shows a schematic of the cross section of this free-jet engine design. An 8° compression ramp upstream of the inlet top surface leading edge is not shown. The 8° compression ramp can be positioned for either ingestion or diversion of the boundary layer (BL). Figure 2 is a photograph of the base regions of the two existing struts which have been extensively tested in a direct connect experiment and will be incorporated into the RBCC engine. These struts each contain three separate rocket chambers, and two hydrocarbon fuel (JP-10) injector wedges. The rocket elements operate on monomethyl hydrazine (MMH) and inhibited red fuming nitric acid (IRFNA). Liquid JP-10 fuel can also be injected through offices in the struts further upstream. The upstream injectors are piloted using small MMH-IRFNA pilots to promote fuel vaporization and ignition. The free-jet airflow is compressed by the 8° ramp, then by the strut leading edges which reach a maximum thickness at the cowl leading edge. There is no internal contraction downstream of the cowl leading edge; although the cross sectional geometry varies, the net cross sectional area is constant. The convergence between the cowl and body-side panels is compensated for by a reduction in strut thickness. This lack of internal contraction enables the inlet to self-start at lower Mach numbers. The non-compressive sidewalls simulate symmetry planes. The combustor and nozzle area variation downstream of the strut trailing edges can be varied manually using the screw-jacks.

During development of the free-jet engine test article, uncertainty in inlet performance and operability emerged as a significant risk to successful strutjet demonstration. A subscale, parametric inlet test was therefore conducted to determine the optimum strut geometry, explore the effect of boundary layer diversion, and quantify the performance and operability of the inlet at the HTF test Mach numbers of 5 and 6. Establishing the cross-sectional flow distribution at the base of the struts was also desired in order to optimize the hydrocarbon fuel injector locations. This paper documents the test program conducted in the NASA Glenn 1- by 1-Foot Supersonic Wind Tunnel (1×1 SWT).

APPARATUS AND PROCEDURE

Sub-Scale Inlet Model

A photograph of the model with the cowl removed, mounted onto the tunnel sidewall is presented in figure 3. The model is uncooled and constructed of carbon-steel. The flowpath is a 40-percent scale version of the inlet for the RBCC freejet engine currently being developed. Figure 4 is a schematic drawing of the model showing the major components. Coordinates of the body and cowl-side surfaces are listed in table I. The model was positioned such that the leading edge of the top surface was either flush with the precompression plate to ingest the boundary layer, or dropped 0.4 in. vertically below the precompression plate for BL diversion. This was accomplished by using shims between the tunnel sidewall and the baseplate of the 8° precompression plate (forebody simulator). With the diverter height set to 0.4 in., the projected capture area is 13.76 in. (ref. 2). The outer sidewalls are flat on the inside surface to simulate symmetry planes. Two identical compression struts divide the flowpath into three channels. The three sets of strut configurations tested are depicted in figure 5. Configurations “A” and “B” reach a maximum thickness at the cowl lip (inlet entrance) plane, resulting in a constant geometric cross-sectional area in all three channels from the cowl lip to the base of the struts. Configuration “A” is tapered from cowl-side to body-side, configuration “B” is untapered. The constant thickness struts (configuration “C”) result in an internal geometric contraction ratio of 1.55. All three strut geometries are 0.90 in. thick by 1.60 in. high, aft of the 8° turn on the body-side (shoulder point). The central channel is 0.94 in. wide while that of the outer channels is 0.49 in. The height of the channels at the inlet shoulder (normal to the body-side surface) is 2.48 in. and 1.60 in. at the strut trailing edge station. Aft of the struts, the flowpath is 2.64 in. wide and 1.60 in. high.

The cowl, body, and compression ramp surfaces of the model are instrumented with a row of static pressure taps along the centerline. The model sidewalls each have a row of static pressure taps at nominally 1 in. spacing on a line halfway between the cowl and body. Table II gives the coordinates of the static pressure taps. A 12-tube pitot pressure rake was used to survey the flowfield exiting all three channels at the base of the struts. The rake traversed from body-side to cowl-side with measurements taken at 20 equally spaced intervals. Of the 12 tubes on the rakes, 6 were used in the center channel and 3 were used in each of the side channels. The rake was translated away from the body-side by a set of thin bars which protruded through the surface directly behind the strut trailing edges, in order to not introduce any additional blockage.

To simulate the back-pressure caused by combustion, a wedge-shaped, hydraulically-actuated mass flow plug was used. At the limit of its forward travel, the tip of the wedge extends to a point corresponding to the trailing edge of the first movable panel in the free-jet engine.

1- by 1-Foot Supersonic Wind Tunnel

The 1×1 SWT (ref. 3) is a one-pass continuous flow facility that can test models from Mach 1.3 to 6.0. The upstream high pressure air is provided by the lab-wide central air services, while the downstream flow is routed to the lab's altitude exhaust system. Figure 6 shows the tunnel circuit as well as facility details. The different Mach numbers are achieved by changing two-dimensional nozzle "blocks"; for the present test program the Mach 4.0, 5.0, 5.5, and 6.0 blocks were used. The tunnel incorporates an electrical resistance heater to bring the air up to elevated temperature. The air is heated to a high enough temperature to prevent condensation in or liquification of the air in the flow. The test conditions properly match the required Mach numbers and Reynolds numbers. The facility stagnation conditions that were run for the various Mach numbers are listed in table III.

Inlet Test Parameters

For each specified set of compression struts, the inlet backpressure (simulated combustor pressure) was varied by translating the mass flow plug. Inlet mass capture was computed independently from four different techniques: employing the mass flow plug data; integrating local mass flow rates determined from static and Pitot pressure measurements at the traversing rake plane; using model dimensions and static pressure measurements at the capture station; and from CFD computations. Boundary layer ingestion or diversion was varied by positioning the precompression plate using steel shims. The compression struts were manually interchanged between test series. Reynolds number variations per Mach number were accomplished by varying the tunnel stagnation pressure and/or the tunnel total temperature.

Inlet Operability Tests

The goal of this program was to select a fixed geometry configuration that consistently and easily self started and provided an acceptable overall inlet performance. Establishing the inlet starting characteristics as a function of freestream Mach for the three different strut configurations was a primary objective. Determining the inlet performance parameters and exit flow uniformity to assess overall flowfield quality at the exit plane was also an important objective. Table IV summarizes the resultant Test Matrix used to satisfy the goal.

To quantify the quality of the flowfield that this inlet provided to the combustor, Pitot pressure, total pressure, Mach number, and mass flow contours were determined for the flowfield at the base of the struts. The Pitot pressure surveys at the inlet exit that along with static pressure measurements at the plane at the base of the struts, were used to compute Mach number contours. The static pressure taps were located 0.38 in. ahead of the traversing rake station, on the centerline cowl and body side of each of the three ducts, and on the outboard sidewalls of each of the outer ducts.

Reynolds numbers effects on inlet performance were recorded; these are aerodynamic effects that primarily manifest themselves through the boundary layer. The Reynolds number was changed by varying either or both the tunnel plenum pressure or the supply airflow line temperature.

Inlet Backpressure Mapping

The mass flow plug was used to determine the maximum pressure that could be maintained in the combustor region before inlet unstart. Inlet operation was characterized from the supercritical condition (plug fully retracted) incrementally through plug translation up to minimum stable operation then on to inlet unstart. As the mass flow plug travel was incremented in the upstream direction, the model exit area was gradually reduced. As the minimum stable point was approached, very fine increments were used to establish a high degree of accuracy when determining the maximum combustor pressure for all configurations. The maximum combustor pressure was established at each Mach number as a function of strut configuration for both boundary layer ingestion and diversion.

RESULTS AND DISCUSSION

Mass Capture and Operability Data

The results of the parametric variations are summarized in table V. The remainder of this paper will focus on configuration B1, the untapered struts with boundary layer diversion, at Mach numbers of Mach 5 and 6. This configuration showed good starting characteristics, was stable, had acceptable flow uniformity, and the best overall inlet performance. This configuration was selected for use in the RBCC engine. Data for all other configurations are available and will be documented.

Inlet mass capture ratios for a started inlet versus freestream Mach are shown in figure 7. The experimental results were calculated from integration of the inlet exit survey data. Theoretical predictions were based on uniform flow and Ames Tables calculations. The NPARC Computational Fluid Dynamics (CFD) code (ref. 4) calculations were made with the following boundary conditions: ideal gas, adiabatic wall, and turbulent flow (k-ε model). Results obtained using the mass flow plug are not shown because large flow non uniformity flowing downstream from the isolator and combustor into the mass flowmeter rendered the mass flow results unreliable. Compared in figure 7 are the theoretical total mass capture (the captured inlet flow (A_o) plus the captured diverter flow (A_d)), the theoretical captured inlet flow (A_o), the experimentally derived captured inlet flow, and the CFD calculated captured inlet flow. The theoretical total captured streamtube was determined from model geometry and dimensions, and from the freestream Mach number dependent pre-compression plate shock angle. The experimentally derived captured inlet flow was determined by computing the required captured inlet area that would provide the massflow computed by the traversing rake at the end of the struts. By subtracting the captured inlet area ratio from the theoretical total captured streamtube ratio, the captured diverter area ratio was determined to be 0.122 at Mach 4, 0.136 at Mach 5, and 0.153 at Mach 6. As is shown, the captured inlet area ratio did not vary significantly at the higher Mach numbers.

Backpressure Data

Static and total pressure inlet data with increasing combustor pressure are shown in figures 8 to 11 for Mach 5 and 6. Figures 8 and 10 show profiles of surface static pressure normalized by freestream static pressure for the model body, cowl, and sidewalls. In order to keep the figures uncluttered, only six cases (I, II, III, IV, V, and VI) are shown out of the large experimental data set. Figures 9 and 11 present corresponding Mach number contours at the base of the struts. The Mach contours are shown are for four cases: a supercritical inlet case, two increasing back pressure cases, and a minimum stable case.

Figure 8 outlines the inlet behavior with increasing back pressures from super critical inlet operation past minimum stable and on to inlet unstart. In the center duct the shock system ahead of the base of the struts is not initially affected by the increasing back pressure; the static pressures in the combustor region rise, but upstream of the combustor the profile has not changed. Subsequent profiles show pressure rises well forward into the isolator and ahead of the inlet shoulder. The minimum stable condition shows the pressure rise near the cowl lip station (maximum thickness station of the struts). These plots show that as the back pressure was increased, the shock system would stop, or stall, on certain sections of the model, such as the end of the struts or the inlet shoulder, before progressing forward again with increasing back pressures. The final, unstarted, profile shows that although the first static pressure tap on the inlet body is at an elevated pressure, the rest of the profile drops. The left sidewall

appeared to experience a classic hard unstart however the right sidewall taps exhibit a profile similar to the middle duct. This indicates that once the left duct has unstarted, sufficient flow was spilled to prevent the other two ducts from unstarting. The pressure dropped in the inlet isolator due to the drop in mass flow through the model resulting from the left duct unstart.

Figure 9 highlights static pressure profile cases I, III, IV, and V, showing the corresponding combustor entrance Mach number flowfield. The supercritical case shows a supersonic flowfield and symmetry between the left and right ducts. Case III confirms what the static pressure profiles indicated in figure 8, that the effect of back pressure is occuring only in the combustor and that the flow ahead of the rake is not being affected. Case IV shows that when static pressure rise occurs ahead of the inlet shoulder the entire flowfield changes and regions of subsonic flow appear on the body side of the duct. The minimum stable case, V, shows a highly distorted flowfield with asymmetric outer ducts. Although most of the duct is subsonic flow, a region of supersonic flow remains near the cowl side of the duct.

Figure 10 outlines the inlet behavior with increasing back pressures at Mach 6. These results are different than those for Mach 5. The shock train moves forward from the combustor through the isolator and into the front of the inlet isolator without getting stalling on sections of the inlet geometry (such as the end of the struts or the inlet shoulder) as occurred at the Mach 5 test condition. Note that the pressure rise is observed forward of the combustor, through the isolator, and near the entrance of the inlet for a stable started case. Another difference with the Mach 5 data is the higher pressure ratio achieved in the combustor (60 percent greater at minimum stable). The one similarity is in the unstarted profile. The unstarted profiles are similar for both Mach numbers because the unstarted left duct causes a pressure rise on the leading edge of the inlet centerline; the static pressure profiles, however, equalize near the shared downstream exit of the isolator.

Figure 11 highlights static pressure profile cases I, III, IV, and V. These Mach number contours concur with the static profiles that the pressure rise through the inlet occurs more gradually at Mach 6 than at Mach 5. The supercritical case I exhibits a supersonic flowfield. Case III shows flow field gradients from subsonic on the body side to supersonic on the cowl side for all three ducts. For Case IV with back pressure, most of the exit profile is subsonic but there is a small sonic/supersonic region near the cowl side for all three ducts. The minimum stable Case V shows a more symmetric flowfield across all three ducts with predominantly subsonic flow and a small sonic core near the cowl side of the center duct.

The overall performance of the B1 configuration at freestream Mach 5 and Mach 6 is summarized in figure 12 which presents kinetic energy efficiency, η_{KE}, versus the Mach number ratio, M_4/M_o at the end of the isolator. The kinetic energy efficiency is given by:

$$\eta_{KE} = \frac{1 - \frac{1}{\eta_{pt}}^{\frac{(\gamma-1)}{\gamma}}}{\frac{(\gamma-1)}{2} M_o^2} + 1$$

where M_4 is the mass averaged Mach number at the end of the isolator as determined by the traversing rake. Note that as the inlet is back pressured η_{KE} decreases until the inlet unstarts before M_4/M_o reaches the sonic value for the Mach 5 case, and M_4/M_o goes under the sonic value for the Mach 6 case.

CONCLUSION

A comprehensive parametric study was conducted to establish the operability and performance of a 40-percent scale inlet for a rocket based combined cycle engine. This study served to demonstrate that the best performance and operability were achieved using a configuration that incorporated nontapered struts, no net internal geometric contraction, and had no boundary layer ingestion (BL diversion). This configuration was therefore selected for use in the RBCC engine. The details of the performance data for this configuration were presented in this paper. This inlet data and flowfield details will help to interpret engine test results and potentially obtain optimized engine performance by providing guidance with fuel injector placement. This study generated an additional data base for a set of modular inlet geometries at Mach 4 to 6. This program served to verify acceptable operability

and performance of a candidate inlet geometry for use with the RBCC engine. This, therefore, eliminated a significant element of risk associated with the upcoming engine test program by providing a very cost effective means of obtaining critical inlet information prior to building the RBCC engine model. This will assure that the inlet will start and achieve good performance during the HTF test, and will provide flowpath performance data to help interpret and streamline the engine test matrix.

REFERENCES

1. Bulman, M.J.; and Siebenhaar, A.: The Strutjet Engine: Exploding The Myths Surrounding High Speed Airbreathing Propulsion. Aerojet Propulsion Division, Sacramento, California, AIAA–95–2475, July 1995.
2. Thomas, S.R.; Woike, M.R.; and Pack, W.D.: Mach-6 Integrated Systems Tests of the NASA Lewis Research Center Hypersonic Tunnel Facility. JANNAF, December 1995 (NASA TM–107083).
3. Skebe, S.A.: Experimental Investigation of Two-Dimensional Shock Boundary Layer Interactions. Ph.D. Thesis, Case Western Reserve University, Cleveland, Ohio, 1983.
4. Cooper, K.: NPARC 2.0-Features and Capabilities. AIAA–95–2609, July 1995.

TABLE I.—RBCC INLET COORDINATES

Description	X, in.	$Y_{BL\ Divert}$, in.	$Y_{BL\ Ingest}$, in.
Compression plate	0	0	0
Inlet leading edge	11.2	2.37	1.97
Strut leading edge	12.04	2.49	2.09
Cowl lip	16.47	5.22	4.82
Inlet shoulder	22.89	3.62	3.22
Strut trailing edge	27.96	3.62	3.22
Inlet trailing edge	34.26	3.62	3.22

TABLE II.—AXIAL COORDINATES OF RBBCC INSTRUMENTATION

Compression plate, in.	Body side, in.	Cowl side, in.	Sidewalls, in.
0.93	12.12	16.96	16.00
4.00	13.36	18.21	17.25
7.07	14.59	19.46	18.49
10.14	15.83	20.71	19.74
	17.07	21.96	20.98
	18.31	23.21	22.22
	19.55	24.46	23.44
	20.78	25.71	24.69
	22.02	26.96	25.97
	23.15	27.68	27.20
	24.40	31.30	27.89
	26.65		31.55
	26.90		
	27.59		
	31.21		
	33.46		

TABLE III.—FACILITY STAGNATION CONDITIONS

M_0	P_{T0}, psia	T_{T0}, R
4.0	40	530
4.0	40	615
5.0	80	686
5.5	150	670
6.0	160	610
6.0	160	765

TABLE IV.—AS TESTED TEST MATRIX

Configuration	Strut/windscreen	Pre-compression plate	M_0	Comments
A1	Tapered	B.L. Diverted	4,5,5.5,6	Acceptable performance
A2	Tapered	B.L. Ingested	5,6	Negligible effect of B.L.
B1	Untapered	B.L. Diverted	4,5,6	Best performance
B2	Untapered	B.L. Ingested	5,6	Negligible effect of B.L.
C2	Constant thickness	B.L. Ingested	5,6	Self start intermittent
D1	No strut	B.L. Diverted	5	Inlet did not start

TABLE V.—RBCC INLET PERFORMANCE SUMMARIZED

Configuration	Mach	Starting	Superscript η_{pt}, η_{KE}	Max p_s/p_{so}	Stable
A1	4.0	Yes	0.38,0.900	19	Yes
A1	5.0	Yes	0.31,0.921	33	Yes
A1	5.5	Yes	0.28,0.927	68	Yes
A1	6.0	Yes	0.26,0.935	73	Yes
A2	5.0	Yes	0.32,0.923	53	Yes
A2	6.0	Yes	0.24,0.930	51	Yes
B1	4.0	Yes	0.53,0.938	22	Yes
B1	5.0	Yes	0.41,0.942	35	Yes
B1	6.0	Yes	0.30,0.943	100	Yes
B2	5.0	Yes	0.41,0.942	46	Yes
B2	6.0	Yes	0.33,0.948	78	Yes
C1	6.0	No	N/A	N/A	N/A
C2	5.0	Difficult	0.40,0.940	34	No
C2	6.0	Yes	0.31,0.945	55	No
D1	6.0	No	N/A	N/A	N/A

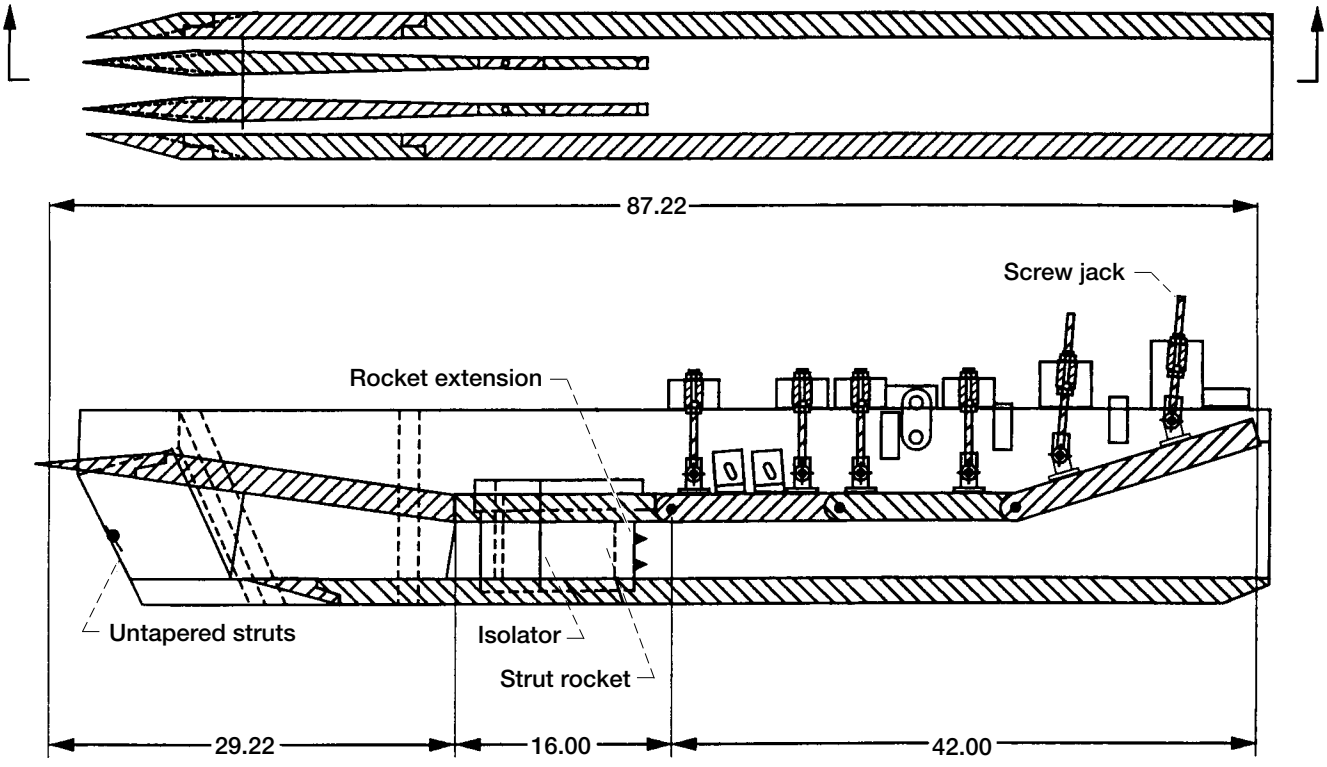

Figure 1.—Strutjet engine test article.

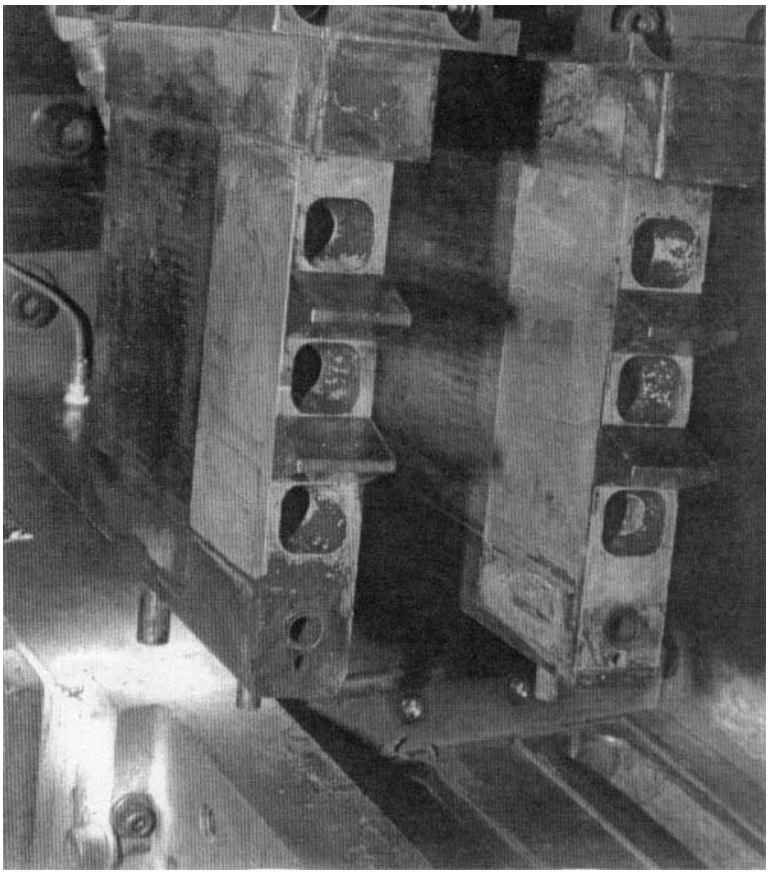

Figure 2.—Rocket chambers and injector wedges on the base region of the two struts.

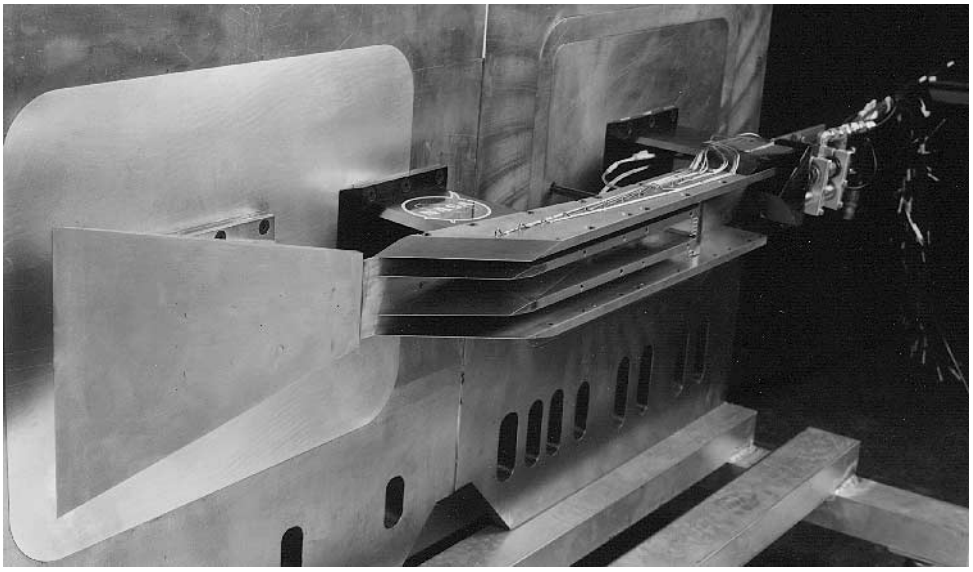

Figure 3.—Forty-percent RBCC inlet model mounted on tunnel sidewall.

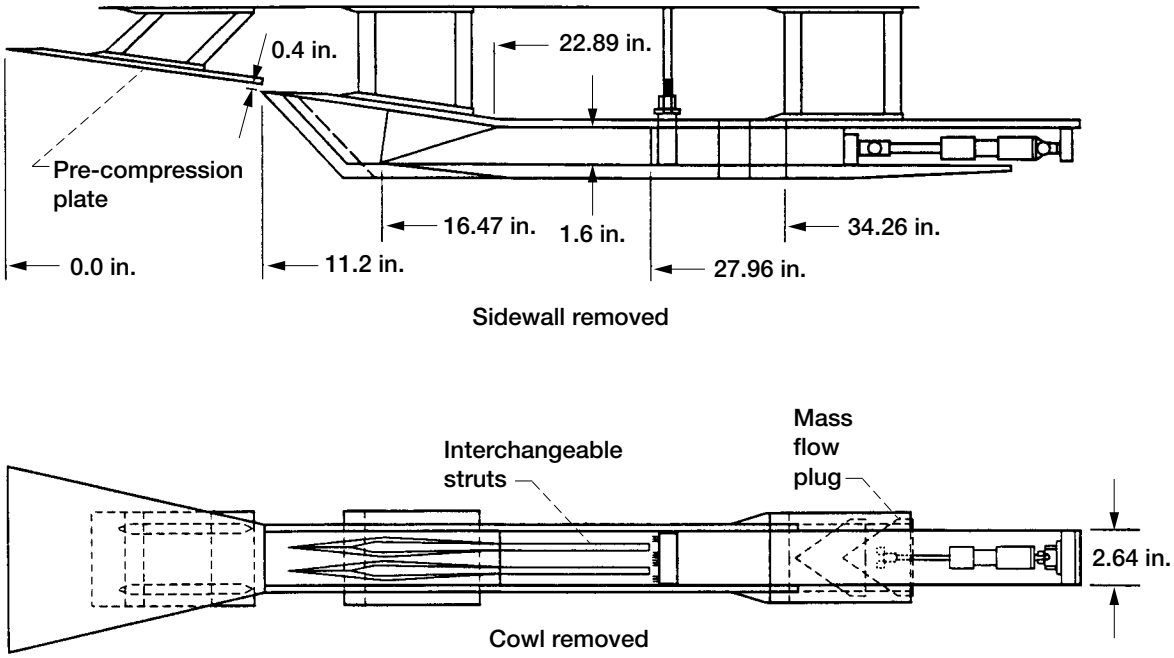

Figure 4.—Sub-scale inlet model.

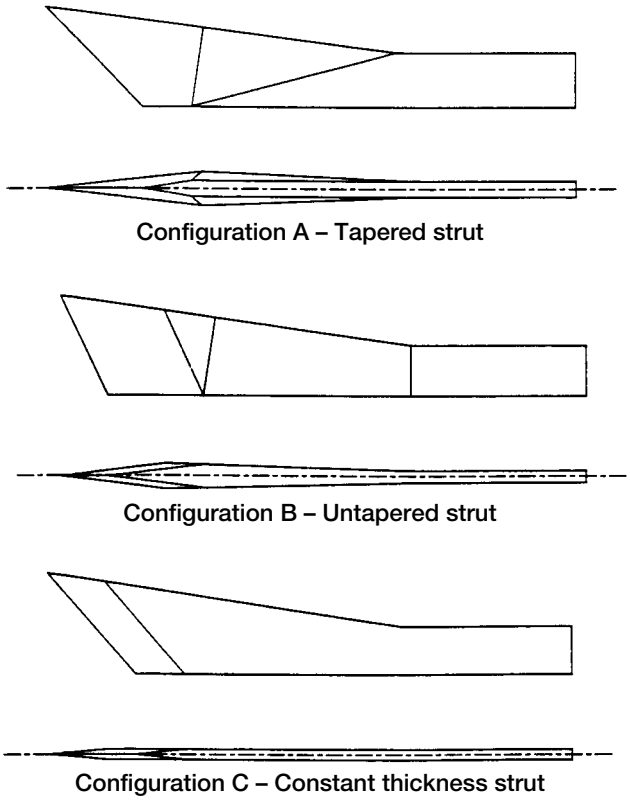

Figure 5.—Three RBCC strut configurations.

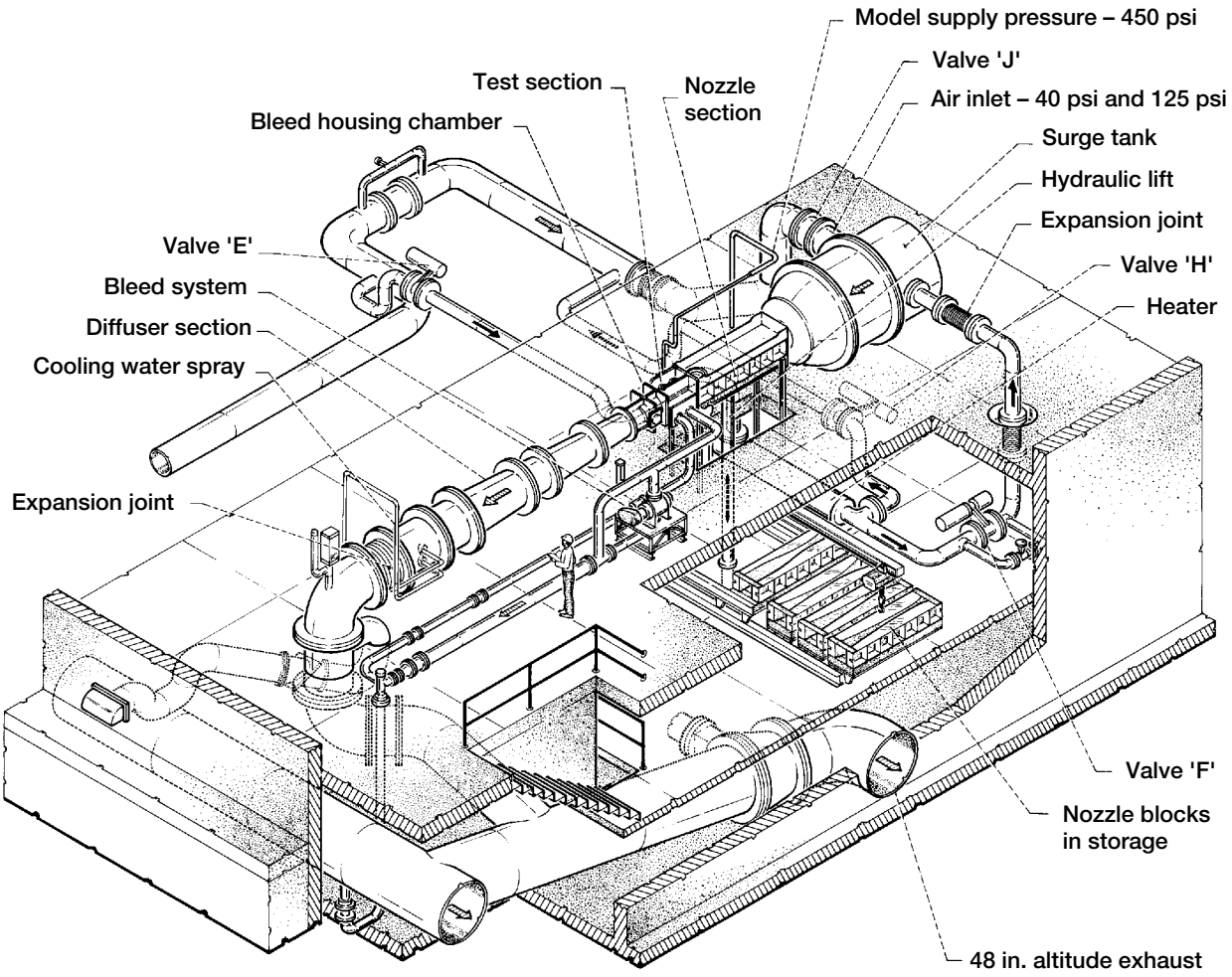

Figure 6.—1- by 1-Foot Supersonic Wind Tunnel, Mach number 1.3 through 6.0, maximum total temperature 650 °R.

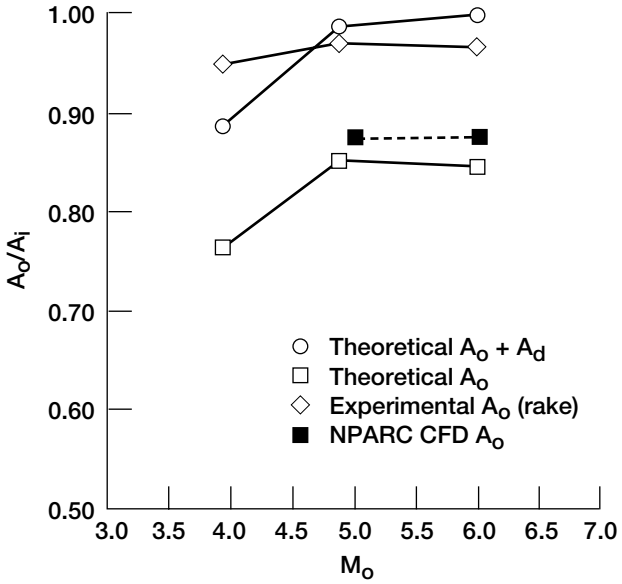

Figure 7.—RBCC inlet captured massflow ratio, configuration B1.

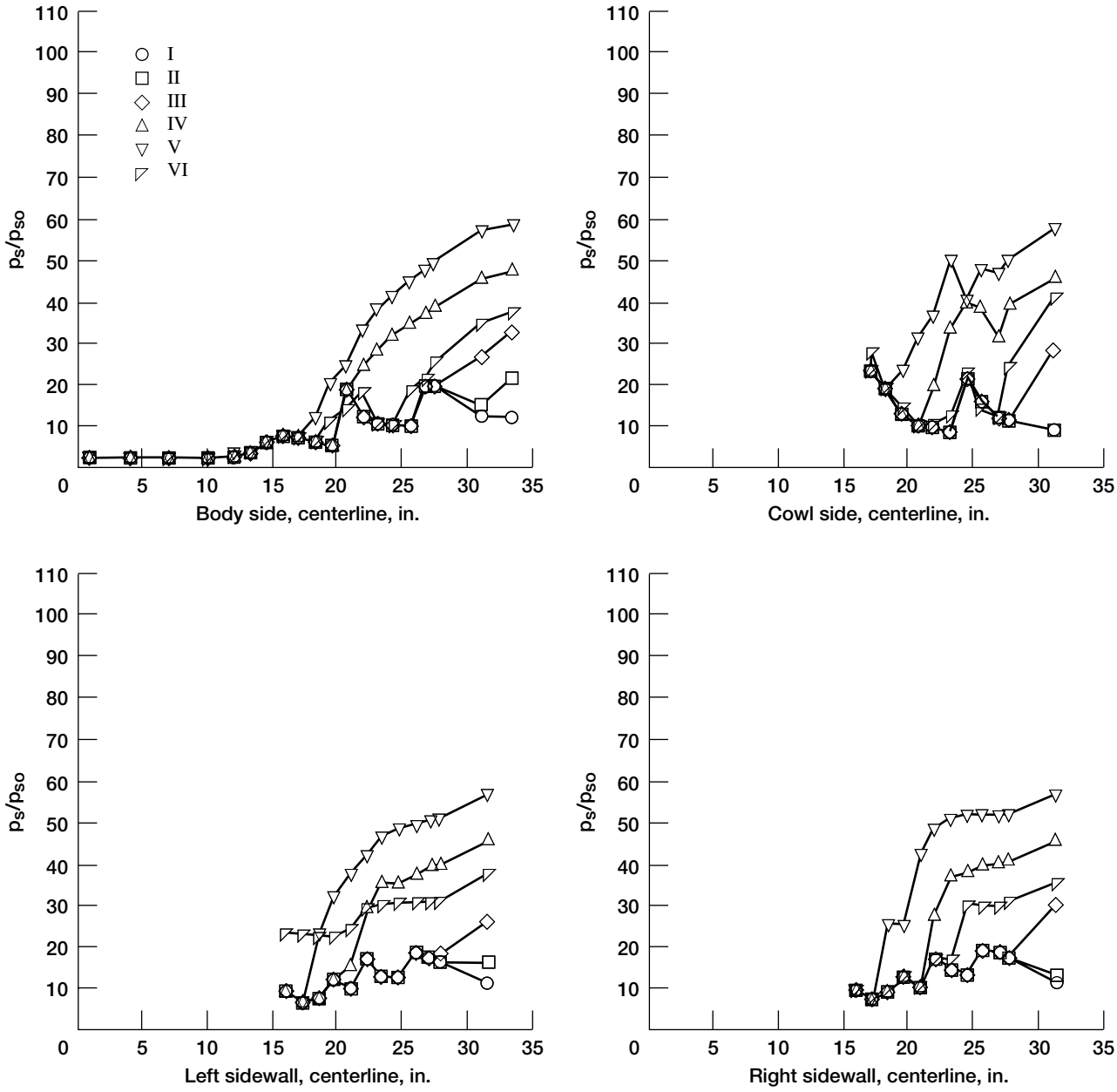

Figure 8.—Model surface static pressure ratios for Mach 5, configuration B1.

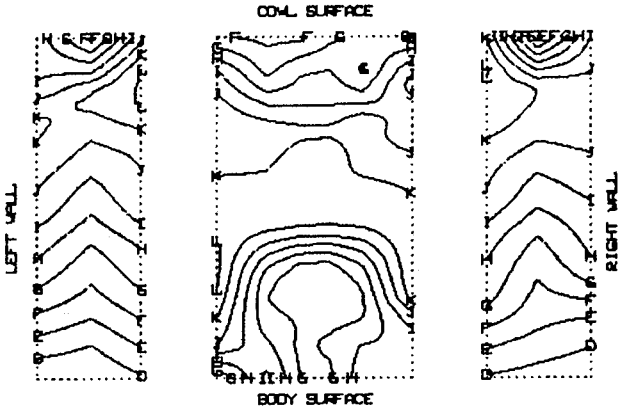

I – p_s/p_{so} = 13.44 (supercritical)

Contour label	Contour value
A	0.000
B	.250
C	.500
D	.750
E	1.000
F	1.250
G	1.500
H	1.750
I	2.000
J	2.250
K	2.500
L	2.750
M	3.000

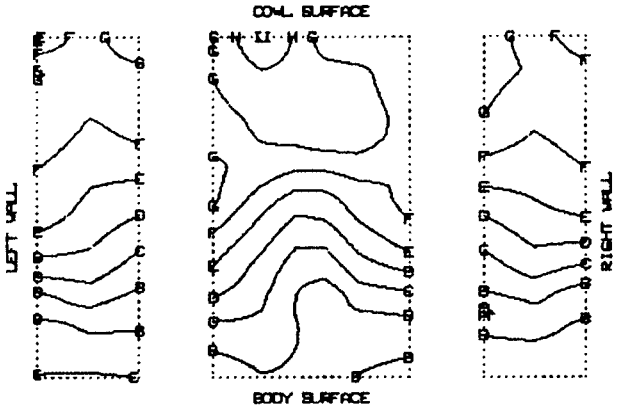

IV – p_s/p_{so} = 51.25 (isolator backpressured)

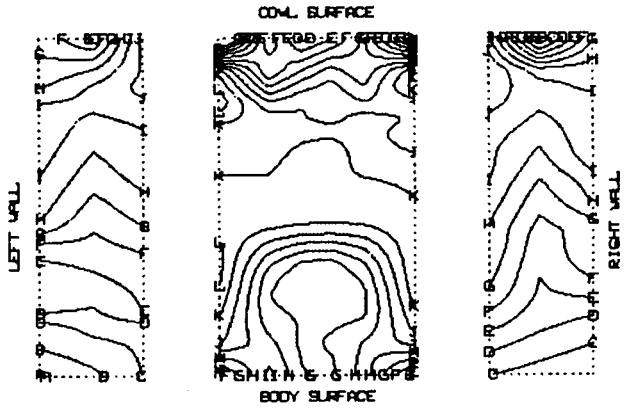

III – p_s/p_{so} = 26.85 (combustor backpressured)

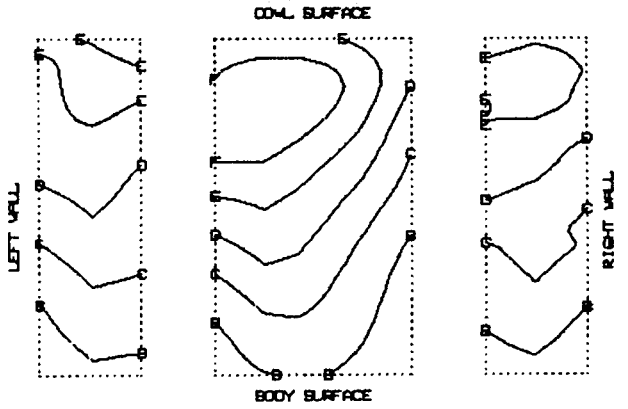

V – p_s/p_{so} = 56.59 (minimum stable)

Figure 9.—Traversing rake plane Mach number contours. Mach 5, configuration B1.

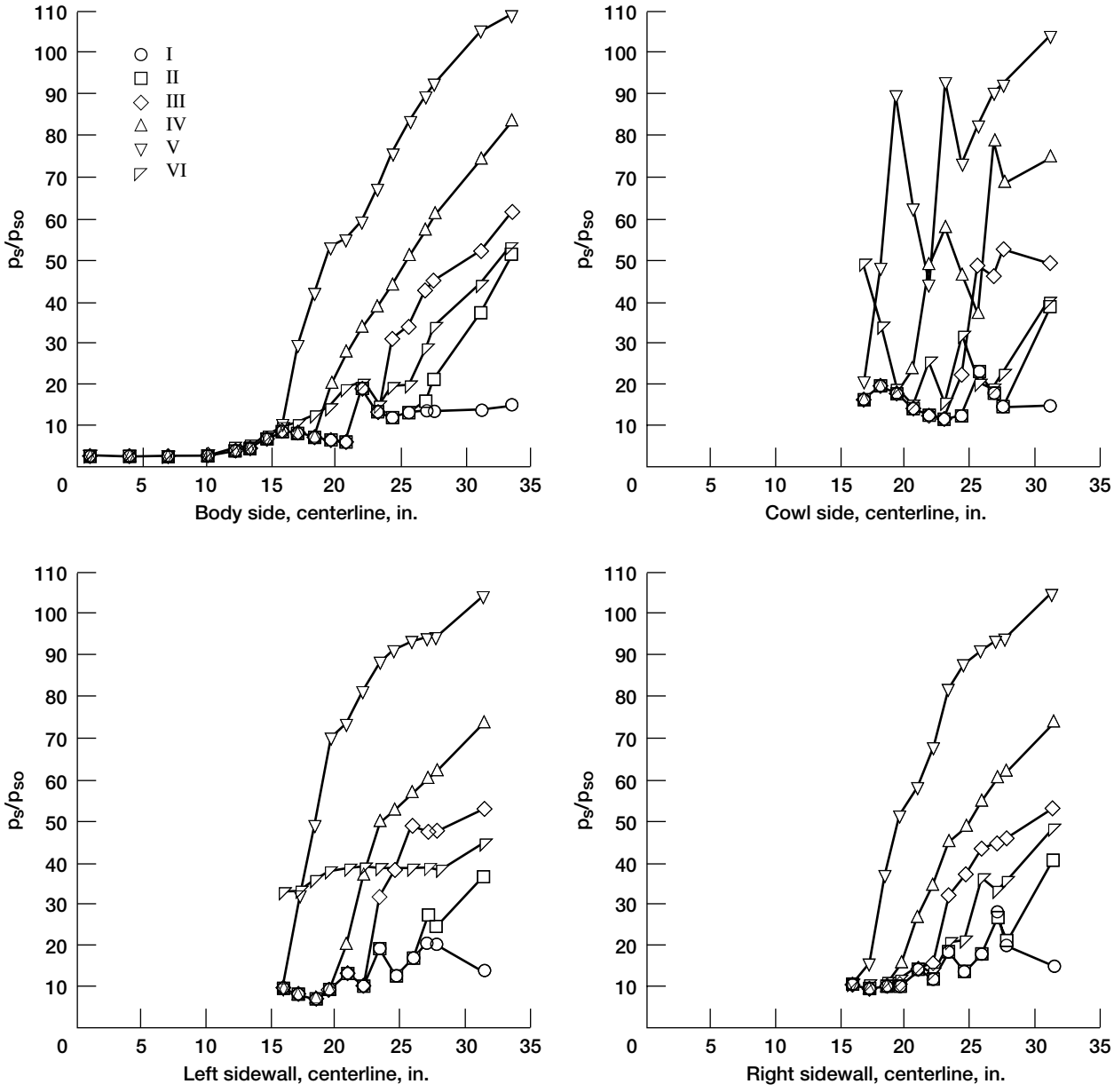

Figure 10.—Model surface static pressure ratios for Mach 6, configuration B1.

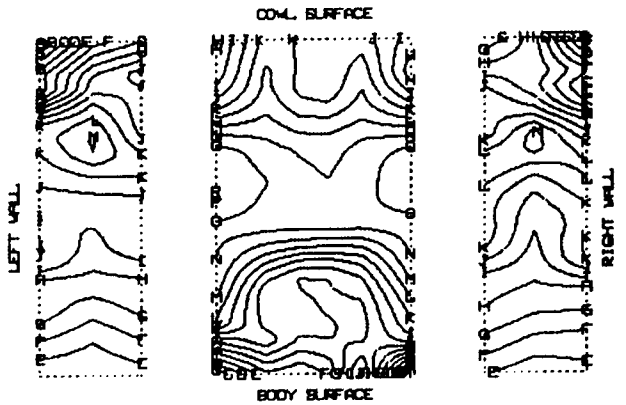

I – p_s/p_{so} = 13.64 (supercritical)

Contour label	Contour value
A	0.000
B	.250
C	.500
D	.750
E	1.000
F	1.250
G	1.500
H	1.750
I	2.000
J	2.250
K	2.500
L	2.750
M	3.000

IV – p_s/p_{so} = 84.79 (isolator backpressured)

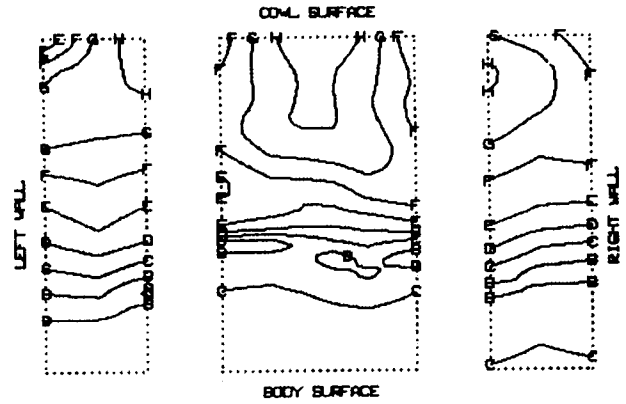

III – p_s/p_{so} = 72.14 (combustor backpressured)

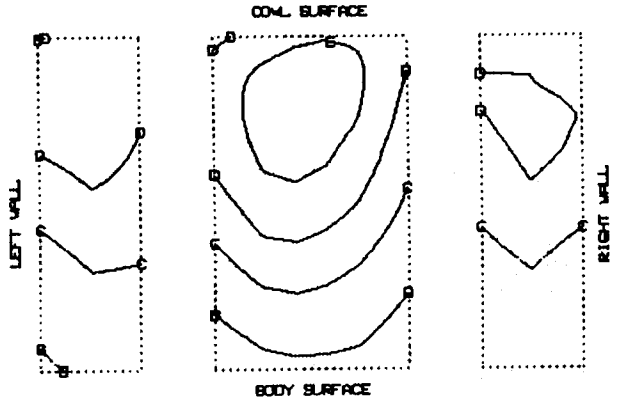

V – p_s/p_{so} = 100.45 (minimum stable)

Figure 11.—Traversing rake plane Mach number contours. Mach 6, configuration B1.

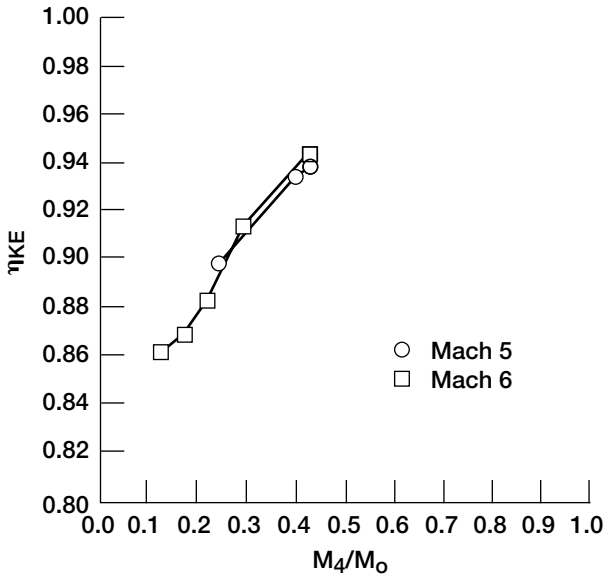

Figure 12.—RBCC inlet performance, configuration B1.

REPORT DOCUMENTATION PAGE

Form Approved
OMB No. 0704-0188

1. AGENCY USE ONLY (*Leave blank*)	2. REPORT DATE	3. REPORT TYPE AND DATES COVERED
	November 2001	Technical Memorandum

4. TITLE AND SUBTITLE

Parametric Data From a Wind Tunnel Test on a Rocket-Based Combined-Cycle Engine Inlet

5. FUNDING NUMBERS

WU–708–48–13–00

6. AUTHOR(S)

René Fernandez, Charles J. Trefny, Scott R. Thomas, and Mel J. Bulman

7. PERFORMING ORGANIZATION NAME(S) AND ADDRESS(ES)

National Aeronautics and Space Administration
John H. Glenn Research Center at Lewis Field
Cleveland, Ohio 44135–3191

8. PERFORMING ORGANIZATION REPORT NUMBER

E–10144

9. SPONSORING/MONITORING AGENCY NAME(S) AND ADDRESS(ES)

National Aeronautics and Space Administration
Washington, DC 20546–0001

10. SPONSORING/MONITORING AGENCY REPORT NUMBER

NASA TM—2001-107181

11. SUPPLEMENTARY NOTES

Prepared for the 1995 Airbreathing Propulsion Subcommittee Meeting sponsored by the Joint Army-Navy-NASA-Air Force Interagency Propulsion Committee, Tampa, Florida, December 5–9, 1995. René Fernandez, Charles J. Trefny, and Scott R. Thomas, NASA Glenn Research Center; Mel J. Bulman, Gencorp Aerojet Corporation, Sacramento, California 95813–6000. Responsible person, René Fernandez, organization code 2780, 1–216–433–6281.

12a. DISTRIBUTION/AVAILABILITY STATEMENT

Unclassified - Unlimited
Subject Categories: 07, 02, and 34 Distribution: Nonstandard

Available electronically at http://gltrs.grc.nasa.gov/GLTRS

This publication is available from the NASA Center for AeroSpace Information, 1–301–621–0390.

12b. DISTRIBUTION CODE

13. ABSTRACT ***(Maximum 200 words)***

A 40-percent scale model of the inlet to a rocket-based combined-cycle (RBCC) engine was tested in the NASA Glenn Research Center 1- by 1-Foot Supersonic Wind Tunnel (SWT). The full-scale RBCC engine is scheduled for test in the Hypersonic Tunnel Facility (HTF) at NASA Glenn's Plum Brook Station at Mach 5 and 6. This engine will incorporate the configuration of this inlet model which achieved the best performance during the present experiment. The inlet test was conducted at Mach numbers of 4.0, 5.0, 5.5, and 6.0. The fixed-geometry inlet consists of an 8° forebody compression plate, boundary layer diverter, and two compressive struts located within 2 parallel sidewalls. These struts extend through the inlet, dividing the flowpath into three channels. Test parameters investigated included strut geometry, boundary layer ingestion, and Reynolds number (Re). Inlet axial pressure distributions and cross-sectional Pitot-pressure surveys at the base of the struts were measured at varying back-pressures. Inlet performance and starting data are presented. The inlet chosen for the RBCC engine self-started at all Mach numbers from 4 to 6. Pitot-pressure contours showed large flow nonuniformity on the body-side of the inlet. The inlet provided adequate pressure recovery and flow quality for the RBCC cycle even with the flow separation.

14. SUBJECT TERMS

Supersonic inlet; Hypersonic inlet; Ramjet; Scramjet; Rocket

15. NUMBER OF PAGES

21

16. PRICE CODE

17. SECURITY CLASSIFICATION OF REPORT	18. SECURITY CLASSIFICATION OF THIS PAGE	19. SECURITY CLASSIFICATION OF ABSTRACT	20. LIMITATION OF ABSTRACT
Unclassified	Unclassified	Unclassified	